LETTER

doi:10.1038/nature11325

Non-classical light generated by quantum-noise-driven cavity optomechanics

Daniel W. C. Brooks[1], Thierry Botter[1], Sydney Schreppler[1], Thomas P. Purdy[1]†, Nathan Brahms[1] & Dan M. Stamper-Kurn[1,2]

Optomechanical systems[1], in which light drives and is affected by the motion of a massive object, will comprise a new framework for nonlinear quantum optics, with applications ranging from the storage[2–4] and transduction[5,6] of quantum information to enhanced detection sensitivity in gravitational wave detectors[7,8]. However, quantum optical effects in optomechanical systems have remained obscure, because their detection requires the object's motion to be dominated by vacuum fluctuations in the optical radiation pressure; so far, direct observations have been stymied by technical and thermal noise. Here we report an implementation of cavity optomechanics[9,10] using ultracold atoms in which the collective atomic motion is dominantly driven by quantum fluctuations in radiation pressure. The back-action of this motion onto the cavity light field produces ponderomotive squeezing[11,12]. We detect this quantum phenomenon by measuring sub-shot-noise optical squeezing. Furthermore, the system acts as a low-power, high-gain, nonlinear parametric amplifier for optical fluctuations, demonstrating a gain of 20 dB with a pump corresponding to an average of only seven intracavity photons. These findings may pave the way for low-power quantum optical devices, surpassing quantum limits on position and force sensing[13,14], and the control and measurement of motion in quantum gases.

Cavity optomechanics has led to powerful applications, including the cooling of massive objects to their motional ground state[15,16] and highly sensitive detection of force and motion. In such systems, displacements as minute as attometers[17] are converted into detectable optical signals, while concurrently the radiation pressure exerted by the light[18,19] strongly modifies the object's oscillations. This disturbance feeds back onto the light field, resulting in high-gain, nonlinear optical parametric amplification. However, observing distinctly quantum optical effects using optomechanical systems has proven elusive. Two such effects have been long-sought goals of optomechanics: the observation of light squeezed by its interaction with a moving mass and the observation of motion driven by light's quantum fluctuations.

In this work, we demonstrate these two phenomena. We establish a novel source of squeezing, generating non-classical light from an optically induced mechanical displacement, and we characterize an optomechanical amplifier driven by quantum fluctuations. Standard methods of generating squeezed light rely on the saturation of a nonlinear medium's electronic energy levels. In contrast, ponderomotive squeezing is predicted to arise when a massive object responds mechanically to quantum optical fluctuations, causing frequency-dependent gain and attenuation of the optical noise spectrum[11,12]. So far, thermal effects of the mechanical bath and optical technical noise have prevented optical observations of a cavity-optomechanical system driven by quantum fluctuations in radiation pressure. Therefore, experiments have focused on simulating ponderomotive squeezing by applying classical optical drives[20,21]. Here we measure a $1.4\% \pm 0.1\% \pm 0.1\%$ reduction in the light's noise power below shot noise. (Throughout this Letter, the first uncertainty is statistical and the second, if present, is systematic.) A thorough examination of statistical and systematic effects (Supplementary Information, section 5) confirms that this noise reduction, although slight, is due to non-classical light and demonstrates ponderomotive squeezing. In comparison with the prediction of the standard linearized theory[22], the actual response of our strongly coupled optomechanical system shows significant differences, suggesting that a nonlinear optomechanical theory[23,24] is required to account for our observations.

We use a cavity-optomechanics system whose mechanical element consists of a cloud of ultracold atoms[9,10]. The atoms are trapped within a few adjacent sites of an optical lattice resonating within a Fabry–Pérot cavity. The atoms are prepared such that the energy of their axial motion is near that of the ground state. The gas couples dispersively to probe light that is nearly resonant with a second cavity mode, detuned by -31 GHz from the atomic D2 resonance. At this detuning, the atoms act as a position-dependent refractive medium, which shifts the cavity resonance frequency. By placing the atoms at lattice sites centred at locations of maximum probe-intensity gradient, we ensure that the probe's cavity resonance frequency varies linearly with the centre-of-mass position of the atoms. When the atoms are centred at these sites, intensity fluctuations in the probe light produce radiation-pressure forces that drive collective atomic motion[25]. By first applying classical modulation to the optical field we demonstrate that the system behaves as a high-gain parametric optomechanical amplifier, using an input pump that feeds just 36 pW of power into the cavity. We then extinguish the classical drive to study the system's response to quantum radiation-pressure fluctuations, mapping the inhomogeneous spectrum of ponderomotive squeezing versus frequency, in both the amplitude- and phase-modulation quadratures of the optical field.

A linearized theory illuminates how ponderomotive squeezing is produced by cavity optomechanics. The optomechanical interaction is encapsulated by the interaction Hamiltonian $\hbar g \hat{a}^\dagger \hat{a}(\hat{b}+\hat{b}^\dagger)$, where $\hat{a}$ and $\hat{b}$ are the annihilation operators for the optical and mechanical fields, respectively (the dagger indicates Hermitian conjugate), g is the optomechanical coupling rate and $\hbar$ is Planck's constant divided by 2π. For small fluctuations, the probe intensity can be linearized about the mean optical field. In this approximation, the cavity-optomechanical system acts as a quadrature-sensitive linear amplifier for optical fluctuations[22]. The steady-state dynamical response of this amplifier at frequency ω, neglecting additional external forces on the mechanical oscillator, is given by the relation between fluctuations in the Fourier-transformed intracavity field $\tilde{a}$ and those of the cavity-filtered input field $\tilde{\zeta}$ (Supplementary Information, section 2). Amplitude fluctuations in the cavity-filtered input field, proportional to $\tilde{\zeta}(\omega)+\tilde{\zeta}^\dagger(-\omega)$, induce motion of the mechanical oscillator, which is then transduced back onto the cavity field with a gain $G(\omega)$:

$$\tilde{a}(\omega)=\tilde{\zeta}(\omega)+\frac{1}{2}G(\omega)\left[\tilde{\zeta}(\omega)+\tilde{\zeta}^\dagger(-\omega)\right] \quad (1)$$

$$G(\omega)\approx\frac{(i\kappa-\Delta)s_{\mathrm{opt}}}{\omega_{\mathrm{s}}^2-\omega^2-i\omega\Gamma_{\mathrm{tot}}} \quad (2)$$

[1]Department of Physics, University of California, Berkeley, California 94720, USA. [2]Materials Sciences Division, Lawrence Berkeley National Laboratory, Berkeley, California 94720, USA. †Present address: JILA, University of Colorado, Boulder, Colorado 80309, USA.

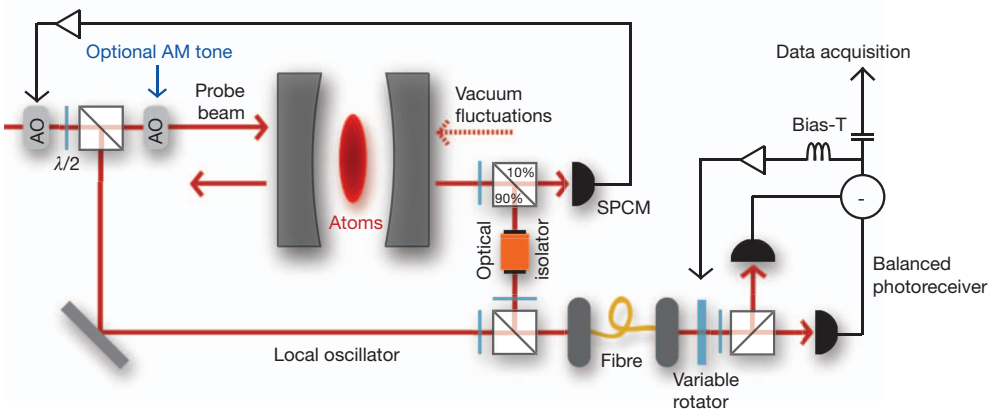

Figure 1 | Schematic of cavity and heterodyne detection set-up. Ten per cent of the cavity output light is diverted to a single-photon counting module (SPCM), and the remainder goes to a heterodyne detector. All beam splitters are polarizing beam-splitter cubes preceded by half-wave plates ($\lambda/2$). The SPCM signal is fed back to control the frequency of an acousto-optic modulator (AO), maintaining a constant probe detuning from the shifted cavity resonance. Additional AOs shift the probe beam 10 MHz relative to the local oscillator and can be used to add amplitude modulation (AM). The probe and local oscillators are mode-matched through a fibre and sent into the detector, which is balanced by controlling the beam polarization with a liquid-crystal rotator.

Here κ is the cavity half-linewidth, Δ is the probe detuning from cavity resonance and $\Gamma_{\mathrm{tot}} = \Gamma_{\mathrm{m}} + \Gamma_{\mathrm{opt}}$ is the combination of mechanical and optomechanical damping. The optomechanical stiffening parameter $s_{\mathrm{opt}} \propto \langle \hat{a}^{\dagger}\hat{a} \rangle g^2$ shifts the mechanical resonance frequency from its unperturbed value, ω_{m}, to $\omega_{\mathrm{s}} = \sqrt{\omega_{\mathrm{m}}^2 + \Delta s_{\mathrm{opt}}}$. When $\Delta = 0$, the transduced optomechanical response appears in the phase of the optical field, and does not interfere with the input radiation-pressure fluctuations. When $\Delta \neq 0$, the gain becomes closed-loop and the optomechanically induced response can interfere destructively with the input fluctuations. When technical and thermal fluctuations are sufficiently small, the ponderomotive suppression of quantum optical fluctuations is resolved as sub-shot-noise squeezing at frequencies near ω_{m}.

For the studies of ponderomotive amplification and squeezing described below, we repeatedly prepare and measure new samples of ~3,500 ^{87}Rb atoms. For each measurement cycle, a microfabricated atom chip delivers the atomic ensemble to two to four adjacent sites of the intracavity optical lattice. Evaporative cooling brings each axial vibrational mode of the gas to near its quantum ground state[26]. The optically bound centre of mass serves as the mechanical element. By controlling the intensity of the optical lattice, $\omega_{\mathrm{m}}/2\pi$ can be changed from a few to several hundred kilohertz. For these experiments, $\omega_{\mathrm{m}} = 2\pi \times 155.5\,\mathrm{kHz}$ is set significantly lower than the cavity half-linewidth, $\kappa = 2\pi \times 1.8\,\mathrm{MHz}$. The optomechanical coupling rate is then $g = (\mathrm{d}\omega_0/\mathrm{d}z)z_{\mathrm{zp}} = 2\pi \times 54\,\mathrm{kHz}$, where $z_{\mathrm{zp}} = \sqrt{\hbar/2m\omega_{\mathrm{m}}}$ is the mechanical harmonic oscillator length, ω_0 is the resonance frequency of the cavity and $m = 0.5\,\mathrm{ag}$ is the total mass of the atomic ensemble.

Because ponderomotive squeezing is observable only when the probe light is detuned from the cavity resonance, we stabilize the probe frequency to $\Delta = -2\pi \times 1.1\,\mathrm{MHz}$. The use of a balanced heterodyne configuration to detect the light transmitted through the cavity reduces the contamination of our measurements by optical technical noise (Supplementary Information, section 5.1). To achieve an overall quantum efficiency of 10.1% for detecting intracavity photons (Fig. 1), we made the cavity mirror on the detector side a factor of eight more transmissive than the input mirror. We restrict the heterodyne signal record to the first 5 ms of probing, after which the atomic sample is significantly heated by radiation pressure fluctuations (Supplementary Information, section 3). In each experimental cycle, we also acquire two additional data streams from the heterodyne receiver: one after the optical cavity is emptied of atoms and one with the probe light extinguished. These record the spectra of technical and shot noise, respectively. The back-to-back recording of squeezed and shot-noise signals every cycle helps eliminate effects of long-term drifts.

We study the optomechanical response to both classical and quantum optical drives. In the first experiment, following recent work[20,21], we measure the classical linear response of the optomechanical amplifier by applying single-frequency amplitude modulation to the input optical field. The complex gain $G(\omega)$ transduces the input modulation onto the amplitude-modulation and phase-modulation quadratures of the optical output field. For each experimental cycle, a single amplitude-modulation tone is applied (Fig. 1). To avoid saturating the response as the drive frequency approaches ω_{m}, the sideband power is reduced from −17 dB to −33 dB with respect to the carrier. Using a superheterodyne technique, we determine the complex response in both quadratures as a function of frequency. The response is characterized (Fig. 2) by a power gain and phase shift relative to the input drive tone, which is independently measured by the empty-cavity data record.

The measured power gain shows regions of strong enhancement of fluctuations (up to 20 dB in power) at frequencies less than ω_{m}. Remarkably, the large gain is achieved with only 36 pW of optical pump power coupled into the cavity, maintaining an average intracavity photon number of seven. This observation suggests that an optomechanical system configured for high input-coupling efficiency could be applied in ultralow-power photonics as an amplifier, filter or switch. At higher frequencies, we observe strong suppression of amplitude fluctuations, with maximal suppression by 26 dB at ω_{m}. The phase shift shows a transition from a delayed to an advanced response, indicated by the response crossing 0° in the amplitude modulation quadrature and −180° in the phase modulation quadrature. The amplifier's stability is maintained because the gain is less than one at the frequencies where there is an advanced response.

Having characterized the ponderomotive optical amplification of our system, we extinguish the deliberate amplitude modulation and drive our system with quantum radiation-pressure fluctuations. Ponderomotive squeezing should result in a strongly squeezed optical field within the cavity with maximal attenuation of ~20 dB at ω_{m} in the amplitude modulation quadrature. Outside the cavity, interference with reflected shot noise shifts the optimally squeezed frequency and quadrature in a Δ-dependent manner[11,12,22]. At our detector, we expect sub-shot-noise squeezing of only a few per cent owing to this interference, optical losses and the heterodyne detector's quantum efficiency. For each run of the experiment, we extract the noise power spectral density (PSD) of the demodulated heterodyne signal. Each cycle of the experiment lasts 40 s, providing a 5-ms-long recording of quantum-noise-driven optomechanical response, as well as empty-cavity and shot-noise records. To obtain sufficient sensitivity to observe low levels of squeezing, we average data from nearly 2,000 cycles of the experiment, yielding a total of 10 s of integration time.

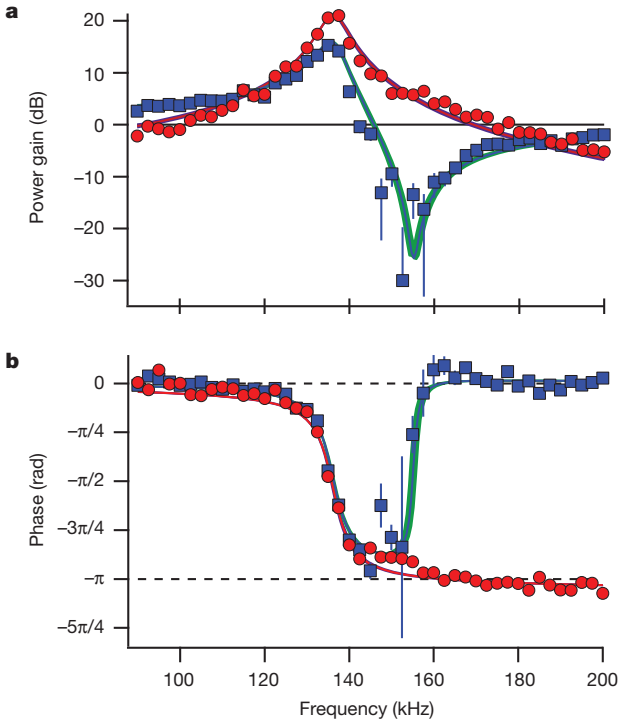

Figure 2 | Optomechanical transduction of classical amplitude modulation. Transduction indicated by the square magnitude of the gain (**a**) and by the phase offset relative to the drive tone (**b**). In the amplitude-modulation quadrature (blue squares in **a** and **b**), the drive is maximally attenuated at ω_m to 26 dB below the response without amplification (horizontal black line in **a**). The drive is also transduced into the phase-modulation quadrature (red circles in **a** and **b**), yielding a strong power response centred at ω_s. At low frequencies, the optomechanical response adds a phase delay. At frequencies greater than ω_m, the optomechanical damping, Γ_{opt}, changes sign, causing the phase offsets of the amplitude- and phase-modulation quadratures to cross 0° and 180°, respectively (dashed lines in **b**). Error bars indicate the measured 1σ statistical uncertainty. The data are in good agreement with the predicted amplitude-modulation response (blue lines) and phase-modulation response (red lines). The effects of systematic uncertainties on the theory are shown in the green and purple shaded regions. By fitting predicted responses to the data, we extract the optomechanically shifted mechanical oscillation frequency ($\omega_s = 2\pi \times 136$ kHz) and the mechanical damping rate ($\Gamma_m = 2\pi \times 1.9$ kHz).

In the PSD, we observe ponderomotive squeezing in the amplitude-modulation quadrature of $1.2\% \pm 0.1\%$ below the measured noise power of uncorrelated vacuum (Fig. 3), without accounting for systematic effects. Correcting for systematic effects (clipping and nonlinear gain in the detection chain, optical power variations, optical path length variations, the detector noise floor and technical noise on the local-oscillator path) the observed squeezing is $1.4\% \pm 0.1\% \pm 0.1\%$ below shot noise, with statistical and systematic errors reported at the 68% confidence level. The measurement is not adjusted for technical noise in the probe path, which also reduces the amount of squeezing observed. The statistical uncertainty arises from an average over the frequency range indicated in Fig. 3. This frequency range is limited by technical optical noise (Brownian noise at low frequencies and additional narrow-band spikes) and by optomechanical response which deviates from the linear theory. To define the limits of the selected frequency range without introducing bias in our analysis of the amplitude-modulation quadrature, we have used independent measurements from the orthogonal phase-modulation quadrature. At frequencies less than ω_s, at a quadrature angle around -40° from amplitude modulation and at frequencies with sufficiently low technical input noise, we observe an additional region of squeezing with the detected noise reduced by $0.8\% \pm 0.2\% \pm 0.1\%$ of shot noise. The overall variation in the PSD with frequency and detection quadrature matches closely with the prediction of the extracavity linear theory of ponderomotive amplification and squeezing (Fig. 3c).

Focusing on frequencies greater than ω_s, we find three features in the PSD that differ significantly from the predictions of linear optomechanical theory. Two of these features are the additional noise peaks at ω_m and $2\omega_s$, which are most significant in the phase-modulation quadrature. The third feature is the level of amplitude-modulation squeezing, which does not reach the 3.7% maximal or 2.4% average (over the indicated range) reduction below shot noise that is expected from linear theory (Fig. 3b) given our system parameters, even after accounting for systematic detection effects. We ascribe these deviations to two causes. The first is the nonlinear wave mixing inherent in the optomechanical interaction, which is predicted to be significant[23,24] in the single-photon strong coupling regime, $g/\omega_m > 1$. Given that in our system $g/\omega_m = 0.35$, we believe that the emergence of the peak near $2\omega_s$ is due to the onset of this nonlinearity. Wave mixing between the Brownian technical noise at low frequencies and the amplified response near ω_s could also contribute to the limited squeezing observed. Nonlinear effects due to single-photon strong coupling will be the subject of future investigation. A second effect is the disturbance of the centre-of-mass mode by the remaining axial mechanical modes of the atomic ensemble, all of which resonate at frequencies near ω_m. These additional modes, which are not sensed directly by the cavity field, serve as the mechanical thermal bath, whose energy exchange with the centre-of-mass mode contributes to Γ_m and may contribute to the noise peak at ω_m.

The ponderomotive squeezing observed in the cavity output spectrum results from coherence between the optical vacuum noise reflected off the cavity mirrors and the radiation-pressure fluctuations driving the intracavity mechanical element. Such squeezing implies that our optomechanical system is dominantly driven by quantum fluctuations in radiation pressure, also known as radiation-pressure shot noise (RPSN). We confirm from the empty-cavity heterodyne record (Supplementary Fig. 3) that, whereas Brownian technical noise contributes significantly to the intracavity fluctuations for $\omega < 2\pi \times 75$ kHz, the noise that drives atomic motion is dominated by shot noise at higher frequencies. This conclusion relies crucially on the fact that only intracavity amplitude-modulation noise contributes to radiation-pressure fluctuations. Accordingly, phase noise inside the cavity does not perturb atomic motion, despite being larger than shot noise by a factor of about ten across the relevant frequency range. (The phase noise is largely common mode to the probe and local oscillator; the residual noise registered by the heterodyne detector is a small fraction of shot noise; see Supplementary Fig. 3.) Whereas previous experiments quantified RPSN bolometrically[25,27], here the dominant role of RPSN can be directly quantified by comparing the observed PSD of the cavity output (Fig. 3) with the values predicted for optomechanical amplification of a pure quantum noise optical input. For instance, at $\omega_s = 2\pi \times 140$ kHz, 97% of the observed phase modulation PSD is expected from RPSN alone, with the remaining 3% resulting from the residual technical, thermal and motional zero-point noise. The close quantitative agreement in frequency regions with large amplification, along with the characterization of squeezing, indicates our observation of both the amplification and suppression of the optical vacuum field due to its interaction with the motion of a mechanical element.

Two key features enable our observations of ponderomotive squeezing and RPSN. First, optical trapping decouples the mechanical element from the surrounding environment. Second, our system operates in a regime where the optical output spectrum is far more sensitive to optical inputs than to mechanical inputs[22]. As a result, nonlinear optical effects such as parametric amplification are observed with extremely weak pump power. Although the observed level of squeezing is small, it nevertheless confirms that optomechanical interactions do indeed generate non-classical light and must be accounted for when using squeezed light to reduce noise in optomechanical force detectors[8]. Established methods for increasing the magnitude of optical

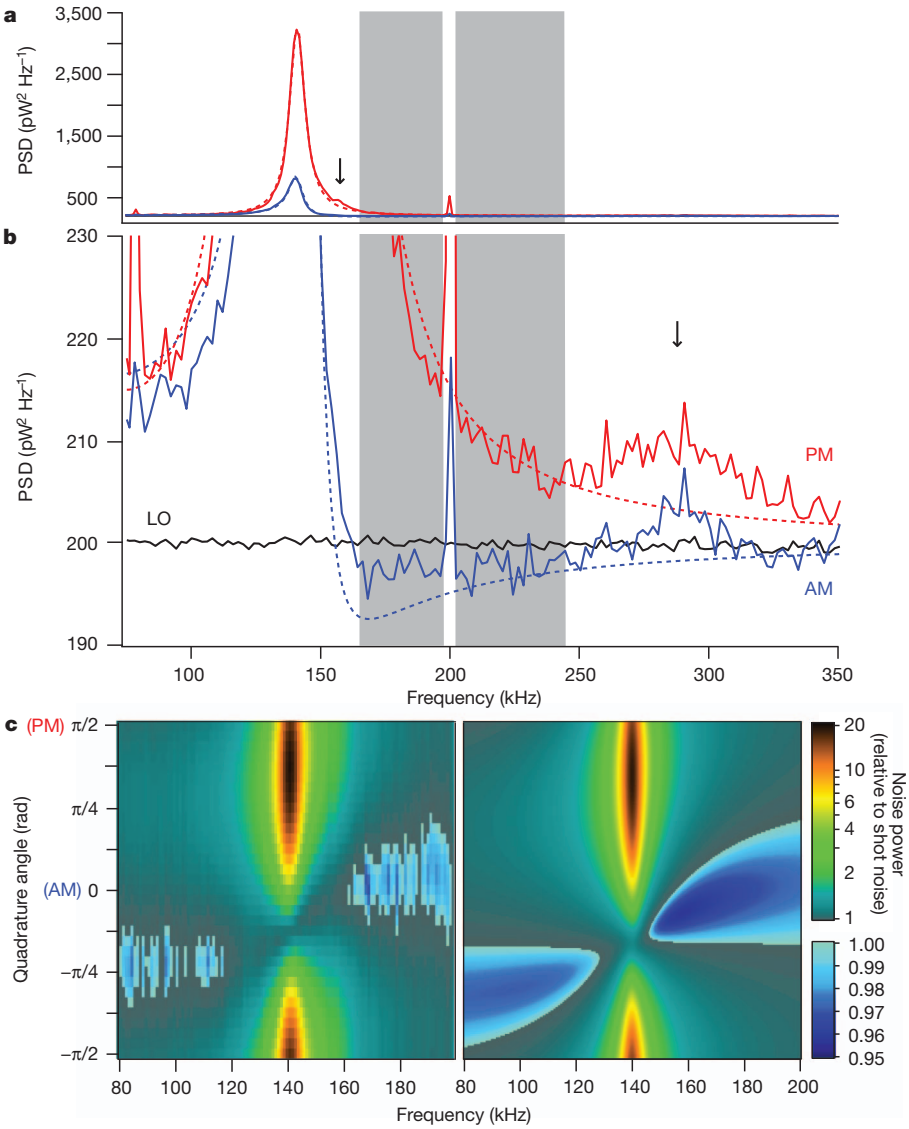

Figure 3 | Ponderomotive squeezing and the optomechanical response to quantum radiation pressure fluctuations. **a**, **b**, Power spectral densities (PSDs) of the optomechanical response are shown with a common abscissa at full scale (**a**) and magnified about the region of shot noise (**b**), in the phase-modulation (PM; red) and amplitude-modulation (AM; blue) quadratures (solid, data; dashed, theory). Theoretical parameters, determined by fitting both the phase-modulation PSD and the technical noise measured in empty-cavity spectra (Supplementary Fig. 3), give the zero-free-parameter amplitude modulation theory line. The local-oscillator PSD (LO; black) determines the shot-noise level. The amplitude-modulation PSD is found to be less than shot noise for frequencies greater than ω_m (grey shaded region). Bounds on the region are identified by a technical noise spike at 200 kHz, and by peaks (black arrows) in the phase-modulation optomechanical response that were not predicted by linear theory. **c**, PSD versus quadrature, shown relative to shot noise. The colour scale changes for squeezed regions. The measured PSD (left) indicates the frequency dependence of the maximally squeezed quadrature and shows overall agreement, especially for regions of amplification, with the linear theory (right), which is shown without technical noise.

squeezing, including implementing homodyne detection, improving detection efficiency and eliminating more low-frequency technical noise, are readily available for future experiments. For a full understanding of ponderomotive amplification, however, our results show that theoretical treatments that go beyond the linear model will be necessary.

Received 5 April; accepted 14 June 2012.
Published online 15 August 2012.

1. Kippenberg, T. J. & Vahala, K. J. Cavity optomechanics: back-action at the mesoscale. *Science* **321,** 1172–1176 (2008).
2. Teufel, J. D. *et al.* Circuit cavity electromechanics in the strong-coupling regime. *Nature* **471,** 204–208 (2011).
3. Weis, S. *et al.* Optomechanically induced transparency. *Science* **330,** 1520–1523 (2010).
4. Safavi-Naeini, A. H. *et al.* Electromagnetically induced transparency and slow light with optomechanics. *Nature* **472,** 69–73 (2011).
5. Safavi-Naeini, A. H. & Painter, O. Proposal for an optomechanical traveling wave phonon–photon translator. *N. J. Phys.* **13,** 013017 (2011).
6. Regal, C. A. & Lehnert, K. W. From cavity electromechanics to cavity optomechanics. *J. Phys. Conf. Ser.* **264,** 012025 (2011).
7. Kimble, H. J., Levin, Y., Matsko, A. B., Thorne, K. S. & Vyatchanin, S. P. Conversion of conventional gravitational-wave interferometers into quantum non-demolition interferometers by modifying their input and/or output optics. *Phys. Rev. D* **65,** 022002 (2001).
8. Corbitt, T. *et al.* Squeezed-state source using radiation-pressure-induced rigidity. *Phys. Rev. A* **73,** 023801 (2006).
9. Gupta, S., Moore, K. L., Murch, K. W. & Stamper-Kurn, D. M. Cavity non-linear optics at low photon numbers from collective atomic motion. *Phys. Rev. Lett.* **99,** 213601 (2007).
10. Brennecke, F., Ritter, S., Donner, T. & Esslinger, T. Cavity optomechanics with a Bose-Einstein condensate. *Science* **322,** 235–238 (2008).
11. Fabre, C. *et al.* Quantum-noise reduction using a cavity with a movable mirror. *Phys. Rev. A* **49,** 1337–1343 (1994).
12. Mancini, S. & Tombesi, P. Quantum noise reduction by radiation pressure. *Phys. Rev. A* **49,** 4055–4065 (1994).
13. Caves, C. M. Quantum-mechanical noise in an interferometer. *Phys. Rev. D* **23,** 1693–1708 (1981).

14. Clerk, A. A., Devoret, M. H., Girvin, S. M., Marquardt, F. & Schoelkopf, R. J. Introduction to quantum noise, measurement, and amplification. *Rev. Mod. Phys.* **82,** 1155–1208 (2010).
15. Teufel, J. D. *et al.* Sideband cooling of micromechanical motion to the quantum ground state. *Nature* **475,** 359–363 (2011).
16. Chan, J. *et al.* Laser cooling of a nanomechanical oscillator into its quantum ground state. *Nature* **478,** 89–92 (2011).
17. Abbott, B. P. *et al.* An upper limit on the stochastic gravitational-wave background of cosmological origin. *Nature* **460,** 990–994 (2009).
18. Braginskii, V. B. & Manukin, A. B. Ponderomotive effects of electromagnetic radiation. *Sov. Phys. JETP* **24,** 653–655 (1967).
19. Caves, C. M. Quantum-mechanical radiation-pressure fluctuations in an interferometer. *Phys. Rev. Lett.* **45,** 75–79 (1980).
20. Marino, F., Cataliotti, F. S., Farsi, A., de Cumis, M. S. & Marin, F. Classical signature of ponderomotive squeezing in a suspended mirror resonator. *Phys. Rev. Lett.* **104,** 073601 (2010).
21. Verlot, P., Tavernarakis, A., Briant, T., Cohadon, P.-F. & Heidmann, A. Backaction amplification and quantum limits in optomechanical measurements. *Phys. Rev. Lett.* **104,** 133602 (2010).
22. Botter, T., Brooks, D. W. C., Brahms, N., Schreppler, S. & Stamper-Kurn, D. M. Linear amplifier model for optomechanical systems. *Phys. Rev. A* **85,** 013812 (2012).
23. Nunnenkamp, A., Børkje, K. & Girvin, S. M. Single-photon optomechanics. *Phys. Rev. Lett.* **107,** 063602 (2011).
24. Rabl, P. Photon blockade effect in optomechanical systems. *Phys. Rev. Lett.* **107,** 063601 (2011).
25. Murch, K. W., Moore, K. L., Gupta, S. & Stamper-Kurn, D. M. Observation of quantum-measurement backaction with an ultracold atomic gas. *Nature Phys.* **4,** 561–564 (2008).
26. Purdy, T. P. *et al.* Tunable cavity optomechanics with ultracold atoms. *Phys. Rev. Lett.* **105,** 133602 (2010).
27. Brahms, N., Botter, T., Schreppler, S., Brooks, D. W. C. & Stamper-Kurn, D. M. Optical detection of the quantization of collective atomic motion. *Phys. Rev. Lett.* **108,** 133601 (2012).

Supplementary Information is available in the online version of the paper.

Acknowledgements We acknowledge C. McLeod for assistance with the manuscript. This work was supported by the AFSOR and NSF. T.B. acknowledges support from the FQRNT.

Author Contributions T.P.P. contributed to the design of the experiment and the development of the theory. All other authors contributed to the design of the experiment, the development of the theory, data acquisition and analysis.

Author Information Reprints and permissions information is available at www.nature.com/reprints. The authors declare no competing financial interests. Readers are welcome to comment on the online version of the paper. Correspondence and requests for materials should be addressed to D.B. (dwb@berkeley.edu).